

Generic Contrast Agents

Our portfolio is growing to serve you better. Now you have a *choice*.



[VIEW CATALOG](#)

AJNR

High-resolution diffusion-weighted MR of fresh and fixed cat spinal cords: evaluation of diffusion coefficients and anisotropy.

P M Pattany, W R Puckett, K J Klose, R M Quencer, R P Bunge, L Kasuboski and R G Weaver

This information is current as of May 20, 2025.

AJNR Am J Neuroradiol 1997, 18 (6) 1049-1056
<http://www.ajnr.org/content/18/6/1049>

High-Resolution Diffusion-Weighted MR of Fresh and Fixed Cat Spinal Cords: Evaluation of Diffusion Coefficients and Anisotropy

Pradip M. Pattany, William R. Puckett, Karl J. Klose, Robert M. Quencer, Richard P. Bunge, Larry Kasuboski, and Raymond G. Weaver

PURPOSE: To use high-resolution diffusion-weighted and calculated apparent diffusion coefficient (ADC) MR imaging to determine whether fixation and storage influence diffusion anisotropy in white matter tracts of cat spinal cord specimens. **METHODS:** Four cat cord specimens were imaged using a diffusion-weighted spin-echo sequence. Diffusion encoding was applied in the section-select axis (parallel to white matter tracts) and in the read axis (perpendicular to white matter tracts). Five sets of axial diffusion-weighted images were acquired with b values ranging from 0 to 800 s/mm² and used to obtain calculated ADC images and to determine diffusion coefficients in different regions of the white matter tracts. **RESULTS:** After cord fixation, a decrease in T2 relaxation and spin density in the white matter caused the signal intensity to appear similar on diffusion-weighted images when the diffusion-probing gradient was applied along both the section-select and read axes. On the calculated ADC images, however, distinct differences in signal intensities were seen in the section-select and read axes. **CONCLUSION:** Although there is little difference in signal intensity in the white matter tracts on diffusion-weighted images when diffusion encoding is applied in the section-select or read axis in the fixed specimens, calculated ADC images confirm that diffusion anisotropy is maintained. Therefore, calculated ADC images may be helpful in the evaluation of fixed spinal cord specimens.

Index terms: Animal studies; Magnetic resonance, diffusion-weighted; Spinal cord, magnetic resonance

AJNR Am J Neuroradiol 18:1049–1056, June 1997

Magnetic resonance (MR) imaging of fresh and fixed postmortem specimens of human and rat spinal cord can show the gross anatomy of the cord both before and after fixation. The T1 and T2 relaxation times and the spin density of gray and white matter are reduced after fixation, but the signal difference between gray and white

matter is preserved in both fresh and fixed specimens (1). Previous studies have shown that comparisons of MR imaging and pathologic findings in spinal cord injury (2–5) are useful in interpreting changes in signal characteristics seen on MR images. However, these comparisons do not reflect the structural integrity of axons in the white matter tracts, which can be seen with diffusion-weighted imaging (6–10).

Molecular diffusion in homogeneous fluid results from a process in which molecules move unrestricted at random (brownian motion), because of thermal agitation. In biological systems, the movement of molecules is restricted by cellular structures. In highly organized biological structures, such as white matter tracts, diffusion properties are said to be anisotropic—that is, diffusion is more restricted in one direction than in another. The changes in MR signal characteristics due to diffusion were shown in 1965 by Stejskal and Tanner (11, 12) with the

Received October 8, 1996; accepted after revision January 17, 1997.

Supported in part by grant NS28059 from the National Institutes of Health, National Institute of Neurological Disorders and Stroke, the Paralysis Project, and the Miami Project to Cure Paralysis.

From the Departments of Radiology (P.M.P., R.M.Q.) and Neurological Surgery (K.J.K., R.P.B.) and the Miami (Fla) Project to Cure Paralysis (W.R.P., K.J.K., R.P.B.), University of Miami School of Medicine; and Picker International Inc, MR Division, Highland Heights, Ohio (L.K., R.G.W.).

Address reprint requests to Pradip M. Pattany, PhD, Department of Radiology, MRI Center, University of Miami School of Medicine, 1115 NW 14th St, Miami, FL 33136.

AJNR 18:1049–1056, Jun 1997 0195-6108/97/1806–1049

© American Society of Neuroradiology

use of a pulsed gradient spin-echo method. Since then, various types of diffusion-weighted imaging methods have been proposed, along with their advantages and limitations (13).

To date, all the studies done with diffusion-weighted imaging have been performed in vivo or on fixed tissue specimens, because diffusion-weighted imaging has the potential to characterize abnormal areas in white matter tracts. Diffusion coefficient values have been measured using calculated apparent diffusion coefficient (ADC) imaging in a fixed rat spinal cord injury model (15). We investigated the effects of fixation and storage on diffusion coefficients along and across the white matter tracts of normal cat spinal cords using calculated ADC images.

Materials and Methods

Four cat spinal cords were imaged within 24 hours of harvesting, depending on availability of the imaging unit, at 1.5 T. The unit has self-shielded gradient coils with 16 mT/m peak gradient strength and a 20 mT/m per second slew rate. A quadrature body coil was used as a transmitter, and a specially designed 4-cm-diameter coil was used as a receiver to provide high-resolution images. The cords were placed in a 4% neutral buffered formalin solution (fixative) for 12 to 14 days and then imaged again. They were then placed in a buffered solution (isotonic salt solution without formaldehyde) for permanent storage, during which they were imaged three times over a period of 31 weeks from the time of the initial study. The cords were stored in the imaging suite, which was kept at a constant temperature of 67°F.

Axial T1- and T2-weighted images were acquired first with a spin-echo sequence and the following parameters: 800/22/5 (repetition time/echo time/excitations) with a 256 × 256 matrix for T1-weighted images; 2000/80/3 with a 220 × 256 matrix for T2-weighted images; 12 contiguous sections, each 3-mm thick, were obtained with a 30-mm field of view; and undersampling of 0.7 was performed along the phase-encode (anteroposterior) axis to reduce the imaging time.

Diffusion imaging was performed using a spin-echo technique, with diffusion-encoding gradients applied on either side of 180° radio-frequency refocusing pulse (Fig 1). The effects of conventional imaging gradients on diffusion cross-terms were minimized by using a gradient-echo waveform for the frequency-encoding (read) gradient and by applying the phase-encoding gradient before collecting the data. Axial diffusion-weighted images were obtained with diffusion encoding applied along the section-select axis (parallel to the white matter tracts, along the z-axis) and read axis (perpendicular to the white matter tracts, along the x-axis). Five different *b* values of 0, 200, 400, 600, and 800 s/mm² were used along each of

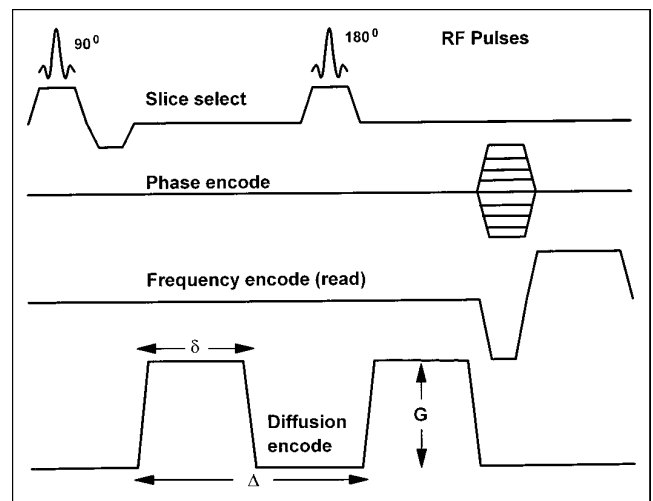


Fig 1. Spin-echo sequence with diffusion-probing gradients of amplitude (*G*), duration (δ), and separation (Δ), which can be applied on any given imaging axis of the spin-echo sequence.

the two axes to obtain calculated ADC images. The diffusion-weighted image parameters were 3000/130/1 with a 256 × 256 image matrix; 12 contiguous sections, each 3-mm thick, were obtained with a 50-mm field of view, and undersampling of 0.7 was performed along the phase-encode axis to reduce the imaging time.

Initial validation of the diffusion-weighted sequence was done by measuring the diffusion coefficient in a 3 × 10-cm cylindrical plastic bottle phantom that contained water doped with CuSO₄ (1.25 g/L).

The amount that the MR signal is attenuated is dependent on the diffusion coefficient of the tissue and the intensity of the diffusion-probing pulsed gradients. Neglecting the term due to conventional imaging gradients, the resulting MR signal attenuation factor (11, 12) is expressed as follows:

$$1) \quad \frac{S}{S_0} = \exp \left[-\gamma^2 G^2 \delta^2 \left(\Delta - \frac{\delta}{3} \right) D^* \right]$$

where *S* is the MR signal when diffusion-probing gradients are applied, *S*₀ is the signal without the application of diffusion-probing gradients, *G* is the amplitude of the diffusion-probing gradient pulses, δ is the duration of the pulses, Δ is the time between their leading edges, and *D*^{*} is the diffusion coefficient of the sample under investigation. The diffusion-sensitive parameter, *b*, is expressed in s/mm² in Equation 2.

$$2) \quad b = \gamma^2 G^2 \delta^2 \left(\Delta - \frac{\delta}{3} \right)$$

Therefore, Equation 1 can now be expressed as follows:

$$3) \quad \frac{S}{S_0} = \exp(-bD^*)$$

For calculating the ADC values, the following expression is used:

$$4) \quad D^* = \frac{\ln\left(\frac{S_0}{S}\right)}{b}$$

For more accurate results, the ADC values were obtained by using five diffusion-weighted images with different b values, and their signal intensities were measured pixel by pixel. A linear regression-fitting algorithm (fitting a straight line to the logarithm of the signal) was used to

obtain the best fit for calculating the diffusion coefficient for each of the 12 sections.

The diffusion-coefficient values were obtained by drawing the regions of interest in the ventral, lateral (left and right sides), and dorsal white matter tracts along with the gray matter regions (left and right sides) (Fig 2) on the calculated ADC images. The mean pixel intensity within each region of interest was calculated by the scanner's computer. The overall analyses were initially performed by using a multivariate analysis of variance (MANOVA) method. Posttest comparisons of individual means were made using the Scheffé method of post hoc comparisons. This method uses a reasonable level of probability ($P \leq .05$) and is powerful for complex comparisons involving more than two treatment means.

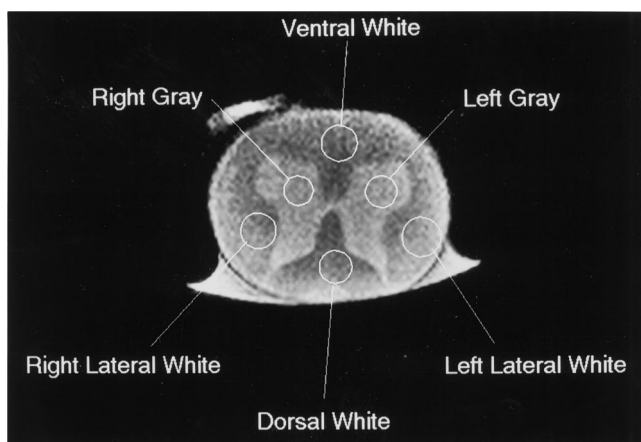


Fig 2. Axial T1-weighted image with typical locations of regions of interest used to obtain diffusion coefficient values from ventral, lateral (left and right sides), and dorsal white matter regions, and gray matter (left and right sides) regions.

Results

Fresh Spinal Cords

In the fresh specimens, both T1- and T2-weighted images displayed similar signal characteristics in gray matter and white matter regions (Fig 3A and B); the gross anatomic structure within the cord was clearly displayed. The diffusion-weighted images acquired of the fresh specimen showed marked differences in signal intensities in the white matter between the two images, indicating there was diffusion anisotropy; the signal in the white matter region was lower than that in the gray matter when the diffusion-probing gradient was applied in the

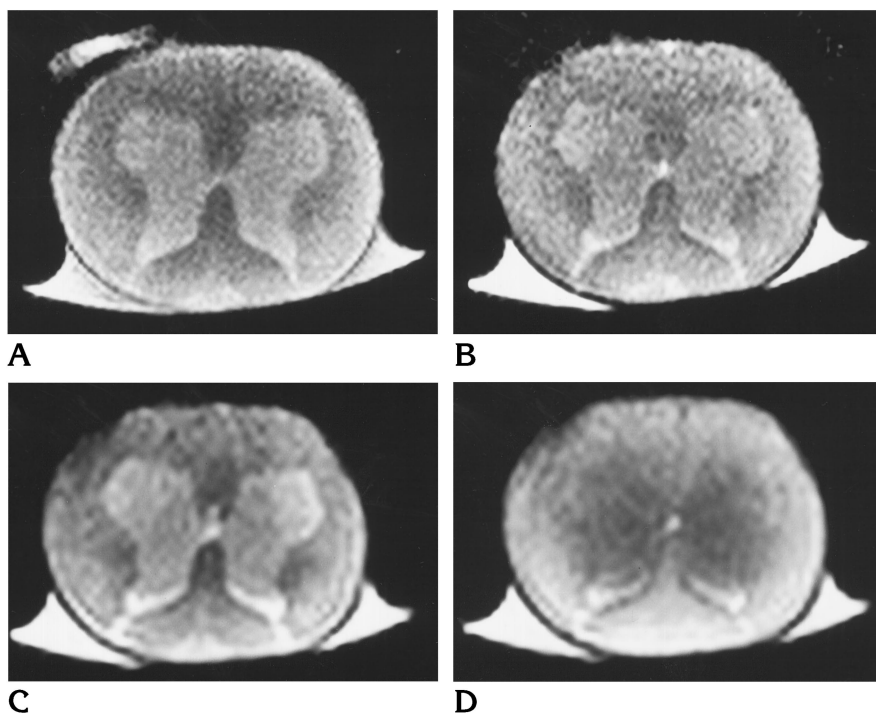


Fig 3. High-resolution axial images of the fresh spinal cord specimen.

A, T1-weighted (800/22/5) spin-echo image shows lower signal intensity in the white matter.

B, T2-weighted (2000/80/3) spin-echo image shows similar gray matter-white matter signal characteristics as the T1-weighted image.

C, Diffusion-weighted (3000/130/1) image with diffusion-probing gradient ($b = 800 \text{ s/mm}^2$) applied in the section-select axis shows the signal in the white matter region is lower than that in the gray matter region.

D, Diffusion-weighted image with diffusion-probing gradient ($b = 800 \text{ s/mm}^2$) applied in the read axis shows the signal in white matter is slightly higher than that in the gray matter.

Fig 4. Calculated ADC images of a fresh cord specimen.

A, Diffusion-probing gradient applied in the section-select axis shows high signal from the white matter regions.

B, Diffusion-probing gradient applied in the read axis shows lower signal from the white matter regions.

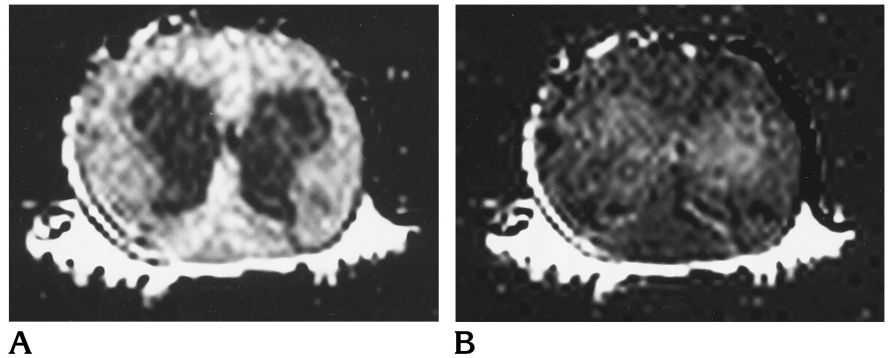
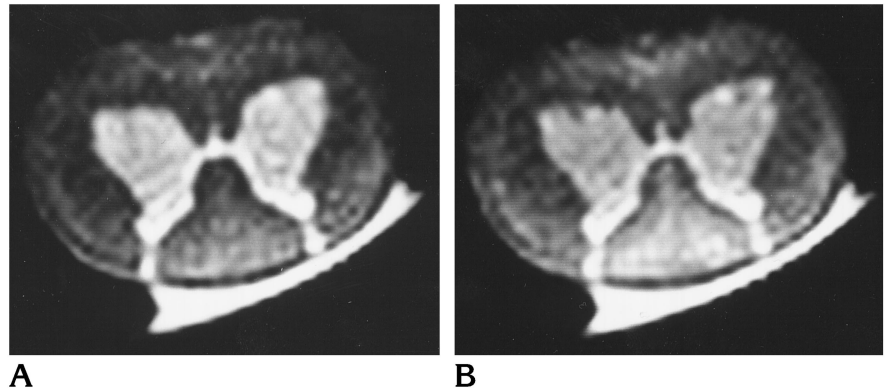


Fig 5. Diffusion-weighted images of a fixed specimen with the diffusion-probing gradient applied in the section-select (A) and read (B) axes. The white matter region has similar signal characteristics in both images.



section-select axis (Fig 3C); the signal in the white matter region was higher than that in the gray matter when the diffusion-probing gradient was applied in the read axis (Fig 3D). Of interest is that the signal intensity at the tips of the gray matter horns was higher on the diffusion-weighted image, and at present we do not have an explanation for this observation. Also, the signal intensity in the lateral and dorsal white matter tracts was higher than that of the ventral white matter tracts on diffusion-weighted images. We believe that this variation is due to a fall-off in the sensitivity of the 4-cm-diameter surface coil. It is more apparent on the long-echo-time diffusion-weighted sequences than the T1- and T2-weighted sequences. The calculated ADC images showed the diffusion anisotropy in the white matter tracts in the fresh specimen when the diffusion-probing gradient was applied in both the section-select (Fig 4A) and the read (Fig 4B) axes. The signal characteristics in the white matter were reversed in the calculated ADC images (Fig 4A and B) as compared with the diffusion-weighted images (Fig 3C and D). In the calculated ADC images, less restricted diffusion (high diffusion coefficient) was depicted as increased signal; for example,

when the diffusion-probing gradient was applied in the section-select axis.

Fixed Spinal Cords

In the diffusion-weighted images of a fixed specimen, the gray matter signal intensity was higher than that of white matter and there was little signal difference in the white matter tracts between the two images when the diffusion-probing gradient was applied in either the section-select (Fig 5A) or read (Fig 5B) axes. The decrease in T2 relaxation in the white matter after fixation and the long (130 millisecond) echo time used to acquire the diffusion-weighted image resulted in increased contrast due to T2 decay. This decay overwhelms the signal changes because of diffusion encoding.

The calculated ADC images showed that the diffusion anisotropy was preserved in the fixed specimen when the diffusion-probing gradient was applied in either the section-select (Fig 6A) or the read (Fig 6B) axis. The images displayed signal characteristics in the white matter that were similar to that seen in the fresh specimen (Fig 3C and D), indicating that diffusion anisotropy was preserved in the fixed specimens.

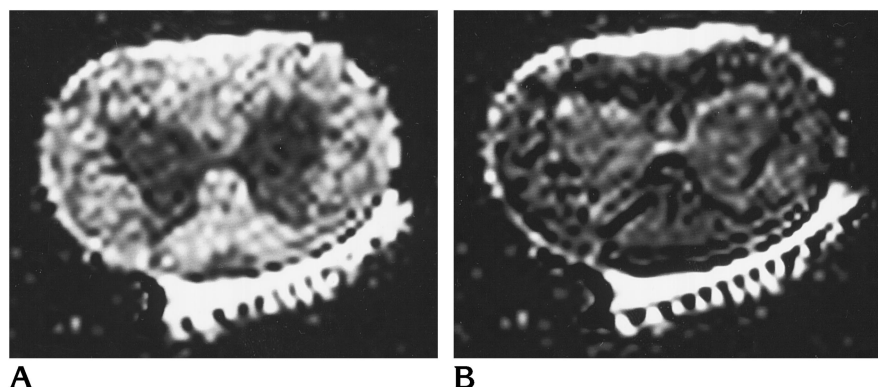


Fig 6. Calculated ADC images of a fixed cord specimen with the diffusion-probing gradient applied in the section-select (A) and read (B) axes. Both images show diffusion anisotropy in the white matter.

Measurements

The diffusion coefficient was measured for the CuSO_4 -doped water solution at 19.4°C (67°F). Values were $1.89 (\pm 0.013) \times 10^{-3} \text{ s/mm}^2$ along the section-select axis and $1.96 (\pm 0.013) \times 10^{-3} \text{ s/mm}^2$ along the read axis. The result corresponded to values observed by Mills (14) at a temperature range of 1°C to 45°C , indicating that ADC values obtained with our method were valid.

After acquiring the calculated ADC images and establishing that these could be used to examine diffusion anisotropy, we evaluated the diffusion coefficients from specific regions within the cord. The values from the gray matter (left and right sides) were averaged and the lateral white matter (left and right sides) were also averaged for each cat cord at a given time point and for a given direction (section-select or read axis) of diffusion probing. Also, results from each cord at each time point (fresh, at fixation, and buffered) were averaged for each of the four regions (ventral white matter, lateral white matter, dorsal white matter, and gray matter region) for a given direction of diffusion probing. The average ADC values for the four cat cords are represented graphically in Figure 7.

The ADC values for the section-select and read axes in each white matter region (ventral, lateral, and dorsal) were dramatically different for each time point, as shown in Figure 7, indicating strong diffusion anisotropy in the white matter regions of spinal cord specimens that were fixed and stored in buffered solution. Similarly, the ADC values were compared in the gray matter regions and found to be significantly different ($P \leq .001$); that is, the values were lower in the section-select axis than in the

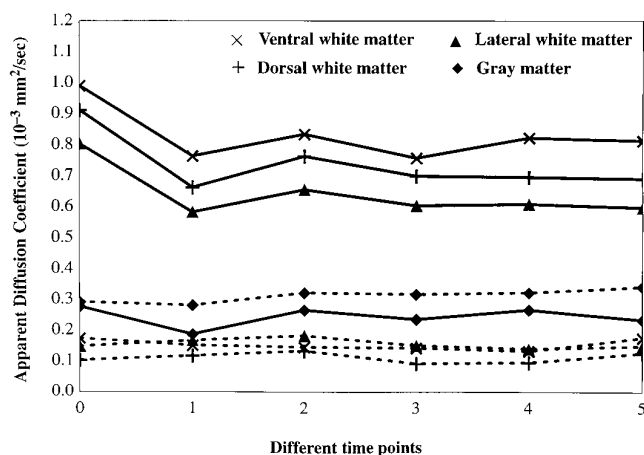


Fig 7. The graph has two curves for a given region, the *solid lines* represent ADC values in the section-select axis and the *dashed lines* represent ADC values in the read axis. The horizontal scale shows the six measurements at different times: 0 = when the cord is fresh, 1 = after 12 to 14 days in 4% neutral buffered formalin solution, 2 = after 2 weeks in buffered solution for long-term storage, 3 = after 4 to 5 weeks in buffered solution, 4 = after 7 to 8 weeks in buffered solution, and 5 = after 30 to 31 weeks in buffered solution.

read axis for each of the measurements shown in Figure 7.

The ADC values in the section-select axis were compared for each region (ventral, dorsal, and lateral white matter, and gray matter) at each time point and were found to be significantly different ($P \leq .001$). However, the ADC values in the read axis were not significantly different between ventral and lateral white matter regions, but they were higher than those in the dorsal white matter region for each time point and lower than those in the gray matter region, as seen in Figure 7.

When we compared ADC values in the section-select axis of fresh cord with those of cord fixed for 12 to 14 days, we found an initial drop

between fresh and fixed cord in the ventral (23%), lateral (27%), and dorsal (27%) white matter regions and in the gray matter region (33%). This change was significantly different ($P \leq .001$). The ADC values in the section-select axis were also compared between cord fixed for 12 to 14 days and all time points of storage in buffer. In the ventral white matter region, the ADC values were not significantly different between those at the time of fixation and those after storage in buffer. In the lateral white matter region, the ADC values at 12 to 14 days' fixation and at 2 weeks' fixation were significantly different ($P = .02$), but the ADC values at more than 2 weeks in buffer were not significantly different from those at 12 to 14 days' fixation. In the dorsal white matter region, the difference in ADC values at 12 to 14 days' fixation and at 2 weeks in buffer was statistically significant ($P = .04$), but a comparison of all ADC values at more than 2 weeks in buffer were not significantly different from those at 12 to 14 days in fixative. In the gray matter region, none of the buffered ADC values were significantly different from the fresh ADC value.

In the read axis, a comparison of ADC values of fresh cord with those at 12 to 14 days' fixation and those stored in buffer showed no significant difference in any of the four regions (lateral, ventral, dorsal white matter, and gray matter).

Discussion

With the use of calculated ADC images, we determined the diffusion coefficient values in the white matter tracts of normal specimens of cat spinal cord as a function of fixation and long-term storage in buffer solution. The results we obtained may be important in future evaluations of spinal cord injury, because this method can characterize abnormal white matter regions in injured or diseased human spinal cord specimens that have been fixed and stored in a buffered solution for long periods of time. The calculated ADC images afford a more sensitive tool for evaluating the structural integrity of white matter tracts, which may not be as well defined with conventional T1- and T2-weighted imaging techniques.

Diffusion-weighted imaging has been used to discern anisotropic restricted diffusion in highly organized structures, such as white matter tracts in the brain and spinal cord (6–10). ADC values have been measured in the white matter

tracts in fixed rat spinal cord injury models to evaluate changes in diffusion anisotropy between normal and abnormal regions (15). It was shown that diffusion was completely isotropic at the epicenter of injury, indicating that there may be mechanical disruption of axons and/or accumulation of extracellular fluid. These researchers postulated that coagulation of proteins caused by formaldehyde would be expected to alter the diffusion characteristics of normal white matter tracts, but they did not investigate the effects of fixation on diffusion imaging. Color-coded diffusion tensor imaging, which uses three-dimensional contrast anisotropy, has been performed to detect alterations in physiological and morphological properties of neuronal fibers in postmortem rat spinal cord after induction of cardiac arrest. It was shown that rapid reduction in anisotropy during the first 2 hours may be caused by changes in axoplasmic flow, and that some degree of anisotropy was retained 4 hours after death depending on the morphological properties of the neuronal fibers (16).

On T1-weighted images, the signal characteristics of gray and white matter of the spinal cord is the opposite of that seen in the brain (Fig 3A): in the spinal cord, the signal of gray matter is higher than that of white matter. Carvlin et al (1), in studies of fresh rat spinal cords, reported that the T1 value of gray matter is slightly shorter than that of dorsal white matter and slightly longer than that of lateral white matter. However, the spin density is much higher in the gray matter than white matter, indicating that the gray matter–white matter contrast is dominated by the higher spin density in the gray matter.

The diffusion-weighted images of the *fresh cord specimens* clearly showed the diffusion anisotropy in the white matter region. The gray matter–white matter signals were well delineated and the signal in the white matter tracts was attenuated when the diffusion-probing gradient was applied in the section-select axis, where the diffusion of water was less restricted (Fig 3C). When the diffusion-probing gradient was applied in the read axis, the signal from the white matter was higher than that from the gray matter, because the diffusion of water was highly restricted (Fig 3D). The calculated ADC images confirmed the observations made on the diffusion-weighted images (Fig 4A and B). The signal from the white matter tracts on the cal-

culated ADC image (Fig 4A) was reversed from that on the diffusion-weighted image, because the diffusion coefficient values were higher when diffusion probing was applied in the section-select axis. As a result, the calculated ADC images displayed high signal intensity in the regions where the diffusion was less restricted. The opposite effect was observed when the diffusion-probing gradient was applied in the read axis, where the diffusion was more restricted in the white matter than in the gray matter (Fig 4B).

The diffusion-weighted images obtained in the *fixed cord specimens* did not show the signal differences observed in the fresh specimens (Fig 5A and B). This was in large part due to the changes in T2 relaxation as a function of fixation and higher spin density in the gray matter. The diffusion-weighted image sequence is influenced by the signal decay due to T2 relaxation because the TE values have to be long in order to apply adequate b values. Carvlin et al (1) reported that the T2 values decreased in fixed human and rat cord specimens by 48% in the white matter and by 28% to 30% in the gray matter as compared with fresh specimens. Also, the spin density in the gray matter was higher than that in the white matter. The relative changes in T2 relaxation and spin density between white matter and gray matter as a function of fixation could effect the signal characteristics observed on fixed diffusion-weighted images. Therefore, it is important to apply a technique such as calculated ADC images to separate the diffusion contrast from T2-dependent contrast and to allow measurements of the diffusion coefficient values (7, 17–19). The calculated ADC images in fixed spinal cord specimens displayed similar signal characteristics as those seen in the fresh spinal cord specimens, confirming that diffusion anisotropy was preserved in the white matter tracts of fixed tissue (Fig 6A and B).

The graph in Figure 7 shows an initial drop in ADC values between fresh cord and that after 12 to 14 days' fixation in the section-select axis (solid lines) in all four regions. This could be due to the cross-linking between the aldehyde and the protein molecules as a function of the fixation process, which would form barriers to the free motion (diffusion) of water molecules along the length of the cord. Also, there is an excess of formaldehyde molecules in the cord that are not bound to the protein molecules,

which could restrict the movement of water molecules.

The ADC values in the section-select axis at 2 weeks in buffer were higher than those after 12 to 14 days' fixation and all the subsequent buffered values. This trend was observed in all regions of the white matter tracts and the gray matter regions (Fig 7). This finding could be attributed to higher concentration of formaldehyde in the cord than in the buffer solution in which it was placed for long-term storage. The difference in formaldehyde concentration would result in an osmotic pressure gradient as a result of water molecules from the buffer solution slowly passing through the permeable membranes of the fixed cord and the formaldehyde molecules leaching out into the buffer solution. Thus, this may represent a temporary hydration effect and its consequences on the ADC values.

The ADC values in the section-select axis of the cord measured at more than 2 weeks in buffer were between those at 12 to 14 days' fixation and those at 2 weeks in buffer. This finding could be due to the formaldehyde concentration being equal in the cord and the buffered solution, resulting in reduced ADC values. The trend toward changes in ADC values as a function of fixation and storage in buffered solution follows a similar pattern for all four regions, as shown in Figure 7.

The data obtained in this study indicate that diffusion anisotropy is maintained in white matter tracts of spinal cord specimens as a function of fixation and long-term storage in buffered solution. Diffusion-weighted images do not display the diffusion anisotropy that is seen on calculated ADC images. We can conclude that calculated ADC images are vital in assessments of the structural integrity of white matter tracts of fixed spinal cord specimens. We may be able to apply the calculated ADC method to fixed cord specimens that have been stored in formaldehyde or buffered solution in order to evaluate structural integrity after spinal cord injury or consequent to any disease process affecting the spinal cord. We believe that this technique will be valuable for future investigators who wish to study detailed anatomic alterations in fixed spinal cords.

References

1. Carvlin MJ, Asato R, Hackney DB, Kassab E, Joseph PM. High-resolution MR of the spinal cord in human and rats. *AJNR Am J Neuroradiol* 1989;10:13–17
2. Becerra JL, Puckett WR, Hiester ED, et al. MR/pathological com-

- parisons of wallerian degeneration in spinal cord injury. *AJNR Am J Neuroradiol* 1995;16:125-133
3. Quencer RM, Bunge RP, Egnor M, Green BA, Puckett WR, Post MJD. Acute traumatic central cord syndrome: MRI-pathological correlation. *Neuroradiology* 1992;34:85-94
 4. Becerra JL, Pucket WR, Marcillo AE, et al. Human spinal cord injury: MRI and histopathology. *Neuroradiology* 1995;37(S):307-309
 5. Duncan EG, Lemaire C, Armstrong RL, Tator CH, Potts DG, Linden RD. High-resolution magnetic resonance imaging of experimental spinal cord injury in the rat. *Neurosurgery* 1992;31:510-517
 6. Moseley ME, Cohen Y, Kucharczyk J, et al. Diffusion-weighted MR imaging of anisotropic water diffusion in cat central nervous system. *Radiology* 1990;176:439-446
 7. Le Bihan D, Lallemand D, Grenier P, Cabanis E, Laval-Jeantet M. MR imaging of intravoxel incoherent motions: application to diffusion and perfusion in neurologic disorders. *Radiology* 1986;161:401-407
 8. Hajnal JV, Doran M, Hall AS, et al. MR imaging of anisotropically restricted diffusion of water in the nervous system: technical, anatomic, and pathologic consideration. *J Comput Assist Tomogr* 1991;15:1-18
 9. Rutherford MA, Cowan FM, Manzur AY, et al. MR imaging of anisotropically restricted diffusion in the brain of neonates and infants. *J Comput Assist Tomogr* 1991;15:188-198
 10. Chenevert TL, Brunberg JA, Pipe JG. Anisotropic diffusion within human white matter: demonstration with NMR techniques in vivo. *Radiology* 1990;177:401-405
 11. Stejskal EO, Tanner JE. Spin diffusion measurements: spin echoes in the presence of a time dependent field gradient. *J Chem Phys* 1965;42:288-292
 12. Stejskal EO, Tanner JE. Use of spin echo in pulsed magnetic field gradient to study anisotropic restricted diffusion and flow. *J Chem Phys* 1965;43:3579-3603
 13. Le Behan D, Turner R, Moonen CTW, Pekar J. Imaging of diffusion and microcirculation with gradient sensitization: design, strategy, and significance. *J Magn Reson Imaging* 1991;1:7-28
 14. Mills R. Self-diffusion in normal and heavy water in the range 1-45°. *J Chem Phys* 1973;77:685-688
 15. Ford JC, Hackney DB, Alsop DC, et al. MRI characterization of diffusion coefficients in a rat spinal cord injury model. *Magn Reson Med* 1994;31:488-494
 16. Matsuzawa H, Kwee IL, Nakada T. Magnetic resonance axonography of the rat spinal cord: postmortem effects. *J Neurosurg* 1995;83:1023-1028
 17. Le Bihan D, Breton E, Lallemand D, Aubin ML, Vignol J, Laval-Jeantet M. Separation of diffusion and perfusion in intravoxel incoherent motion (IVIM) MR imaging. *Radiology* 1988;168:497-505
 18. Thompson C, Henriksen O, Ring P. In vivo measurement of water self diffusion in human brain by magnetic resonance imaging. *Acta Radiol* 1987;28:353-361
 19. Chien D, Buxton RB, Kwong KK, Brady TJ, Rosen BR. MR diffusion imaging of the human brain. *J Comput Assist Tomogr* 1990;14:514-520